Supporting Figure 1:

1D traces along ω_1 taken at the proton frequency of Phe4 from a $^1H,^{13}C$-HSQC[13] spectrum of ^{13}C, ^{15}N labeled human ubiquitin in 500 µl 90% H_2O, 10% D_2O recorded on a four-channel BRUKER DRX600 spectrometer at a temperature of 303 K. a) Experimental performance of synchronous HS2 homonuclear decoupling of ^{13}C with a decoupling RF amplitude $\gamma B_1/2\pi^{max}$ = 6720 Hz. The sideband intensities at $(\tau_p)^{-1}$ = 250 Hz have a relative intensity of 32.8% with respect to the centerband. b) Experimental performance of synchronous HS2 homonuclear decoupling of ^{13}C with a decoupling RF amplitude $\gamma B_1/2\pi^{max}$ = 4800 Hz. The sideband intensities have a relative intensity of 17.3%. c) Experimental performance of synchronous HS2 homonuclear decoupling of ^{13}C with a decoupling RF amplitude $\gamma B_1/2\pi^{max}$ = 3360 Hz. The sideband intensities have a relative intensity of 9.5%. d) Experimental performance of asynchronous HS2 homonuclear decoupling of ^{13}C with a decoupling RF amplitude $\gamma B_1/2\pi^{max}$ = 3360 Hz. The quality of the decoupling is largely enhanced.

Supporting Figure 2.

Variations of crystallographic ω_i^* torsion angles along the peptide sequence. The torsion angle ω is phase shifted in order to visualize the slight deviations from idealized *trans* conformations ($\omega_i^* = 0°$).

Supporting Figure 3.

Normalized $^{13}C_\alpha$ reference peak intensities obtained from the proposed quantitative J correlation HN(COCA)CA experiment as a function of the peptide sequence.

Supporting Table 1.

Values of extracted $^{3}J(C_{\alpha},C_{\alpha})$ coupling constants for ubiquitin

Supporting Table 2.

Values of extracted and predicted $^{3}J(C_{\alpha},H^{N})$ coupling constants for ubiquitin

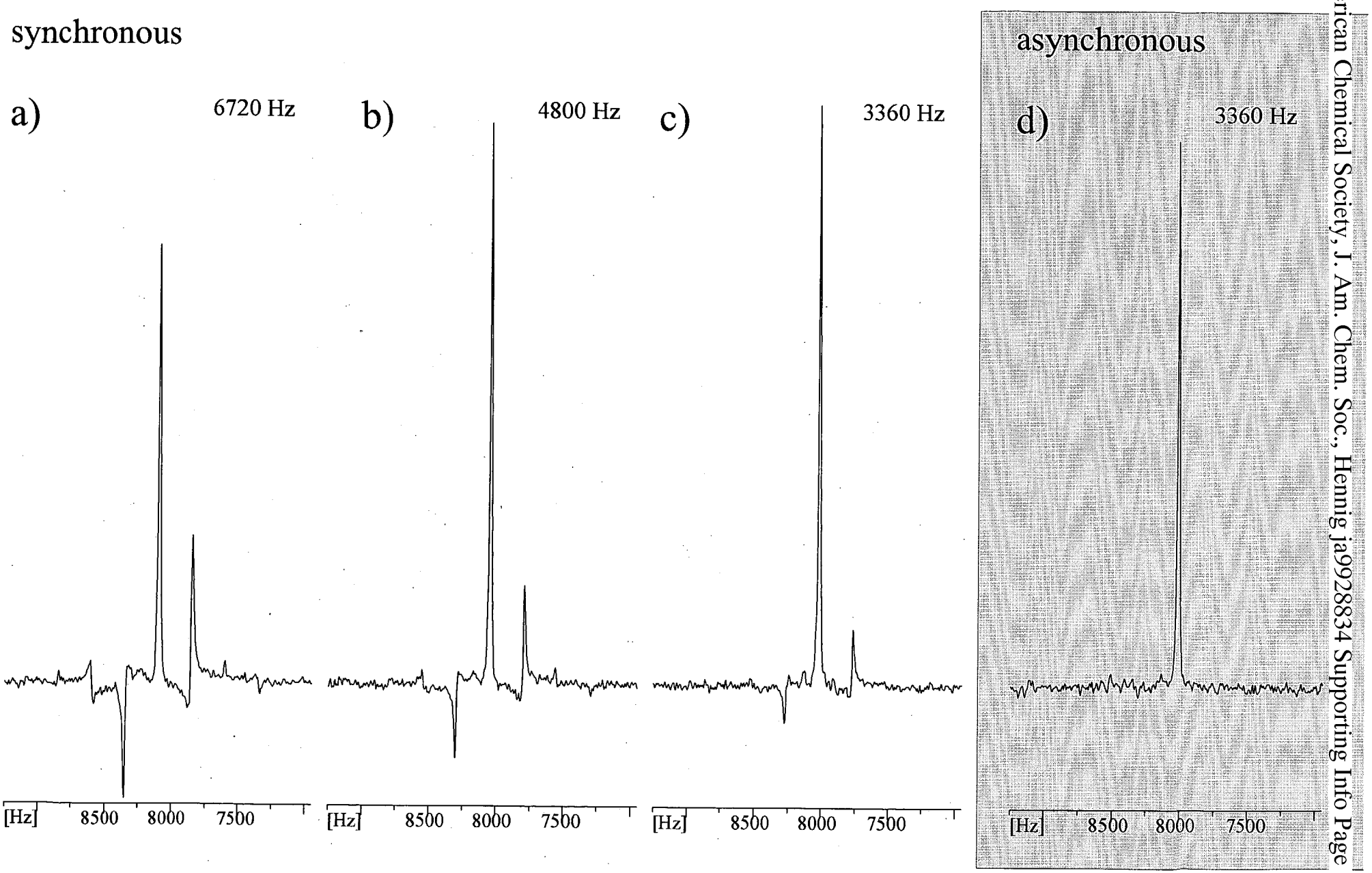

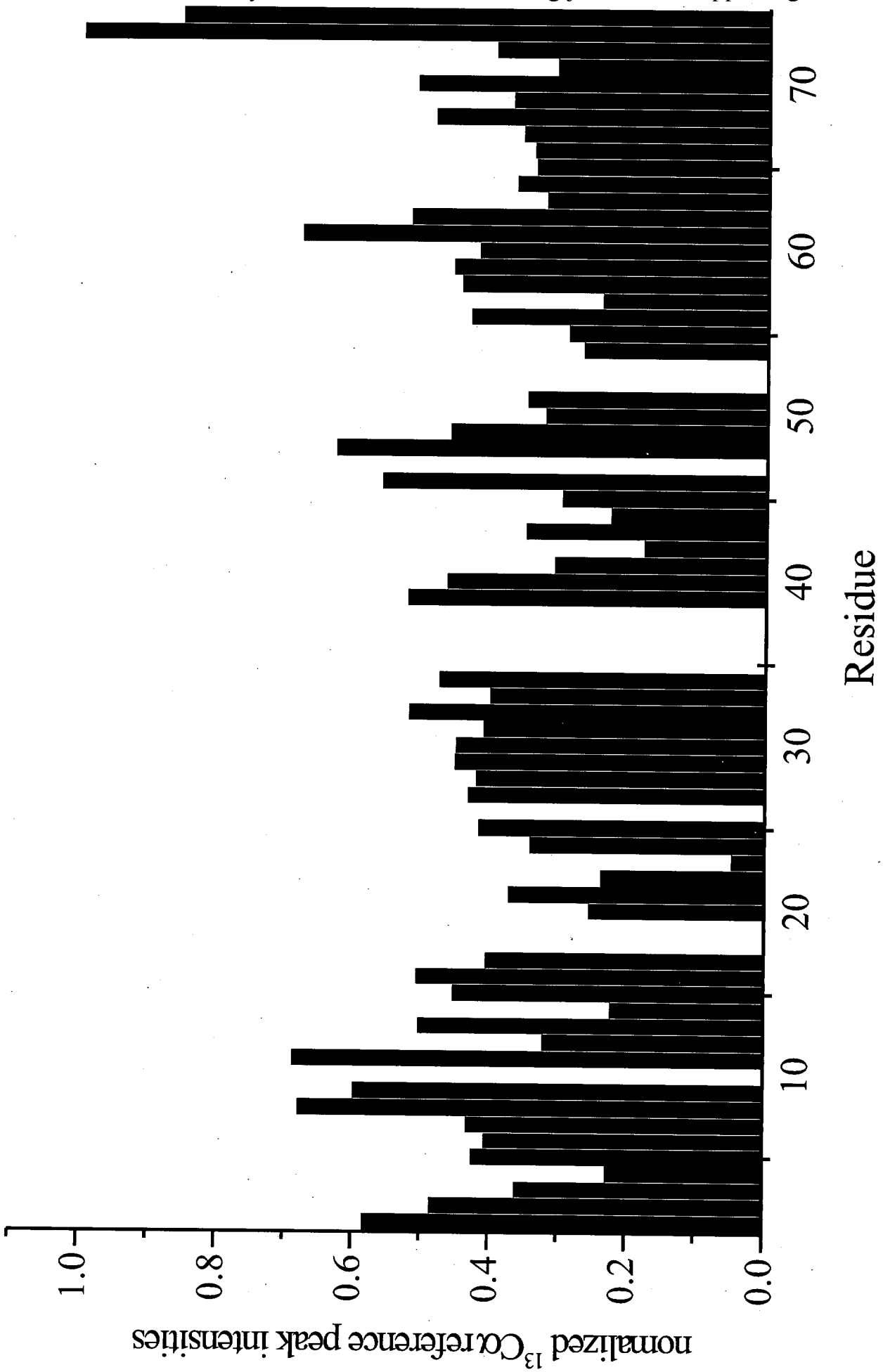

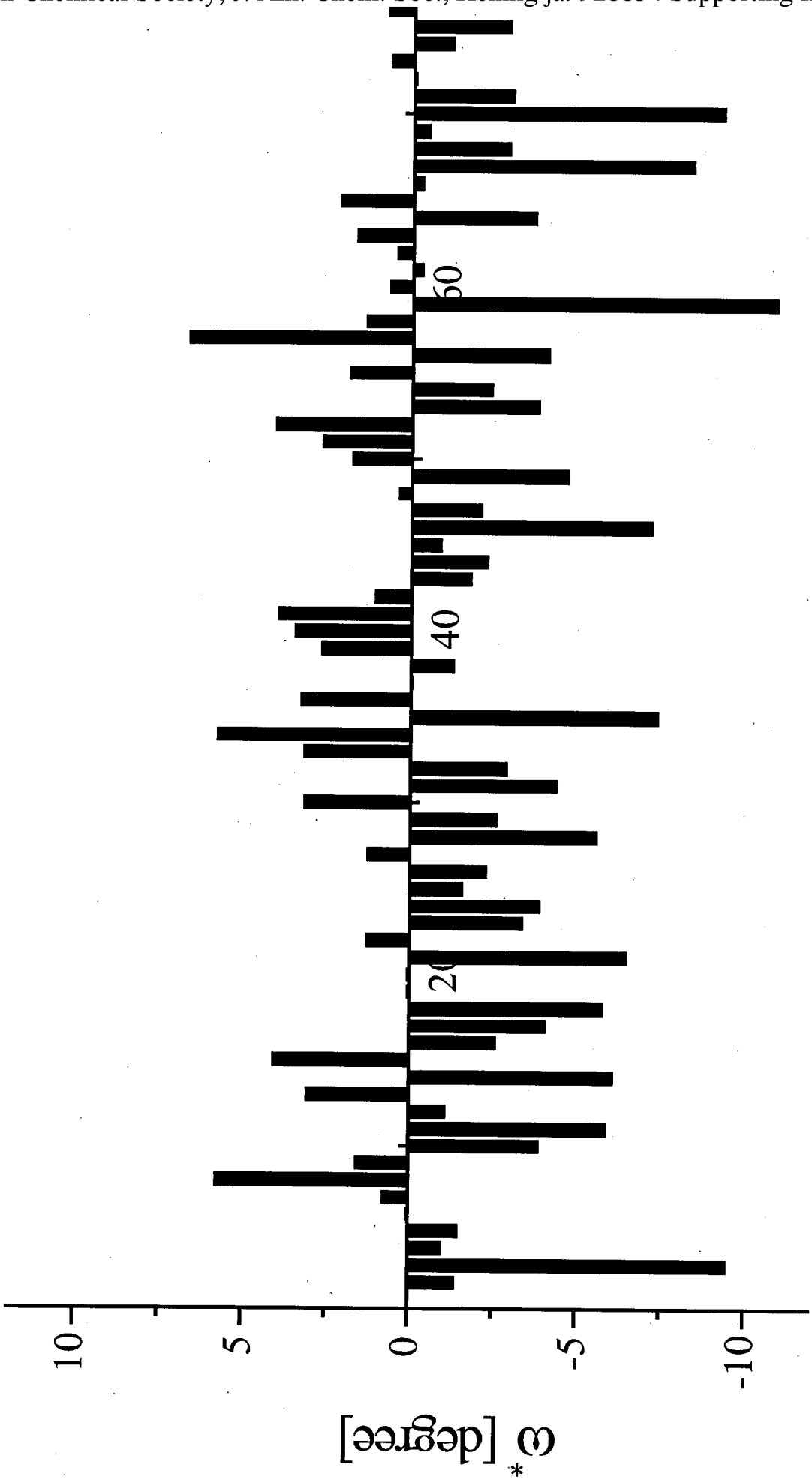

Supporting Table 1

Values of extracted $^3J(C_\alpha,C_\alpha)$ coupling constants for the ubiquitin

residue	$^3J(C_\alpha,C_\alpha)$ [Hz][a]	rmsd [Hz][b]
Met1		
Gln2	2.18	0.05
Ile3	1.83	
Phe4	1.87	
Val5	1.65	0.00
Lys6	1.54	
Thr7	1.75	
Leu8	1.35	
Thr9	1.05	0.32
Gly10		
Lys11		
Thr12	1.64	0.06
Ile13	1.61	
Thr14	1.50	
Leu15	1.68	0.05
Glu16	1.63	0.01
Val17	1.79	0.11
Glu18	1.59	
Pro19		
Ser20		
Asp21		
Thr22	1.62	0.16
Ile23	1.60	
Glu24	<1.0	
Asn25	<0.9	
Val26		
Lys27	<0.9	
Ala28	<0.9	
Lys29	<0.8	

Ile30	<0.8	
Gln31	<0.9	
Asp32	<0.8	
Lys33	<0.9	
Glu34	<0.8	
Gly35		
Ile36		
Pro37		
Pro38		
Asp39	<0.8	
Gln40	<0.8	
Gln41		
Arg42	1.75	
Leu43	1.52	0.12
Ile44	1.86	0.06
Phe45	1.53	0.04
Ala46	1.76	0.11
Gly47		
Lys48		
Gln49	1.73	
Leu50		
Glu51	1.65	
Asp52	2.05	
Gly53		
Arg54		
Thr55	1.71	0.09
Leu56	1.46	0.04
Ser57		
Asp58		
Tyr59		
Asn60	1.07	
Ile61	1.07	

Gln62	1.64	
Lys63	1.70	
Glu64	1.84	
Ser65		
Thr66	1.57	
Leu67	1.67	0.11
His68	1.66	
Leu69	1.82	
Val70	1.65	
Leu71		
Arg72	1.87	
Leu73	1.95	0.09
Arg74	1.44	0.01
Gly75		
Gly76		

[a] Values of $^{3}J(C_{\alpha},C_{\alpha})$ were determined from the ratio of reference and the cross peak intensities as described in the text. [b] Pairwise root-mean-square (rms) difference of $^{3}J(C_{\alpha},C_{\alpha})$ coupling constant values measured twice, once starting from $^{13}C_{\alpha i}$ and detection of the cross peak intensity at the frequency of $^{13}C_{\alpha i-1}$, and once vice versa. Maximum values of unobserved $^{3}J(C_{\alpha},C_{\alpha})$ couplings are determined from the intensity ratio of the smallest cross peak observable and the corresponding reference intensity. Coupling constant values are not corrected for $^{13}C_{\alpha}$ spin flips.

Supporting Table 2

Values of extracted and predicted $^3J(C_\alpha,H^N)$ coupling constants and crystallographic torsion angles for ubiquitin

residue	ϕ_i [degree]	ψ_{i-1} [degree]	$^3J(C_\alpha,H^N)$ exp. [Hz][a]	$^3J(C_\alpha,H^N)$ pred. [Hz][b]	$^3J(C_\alpha,H^N)$ pred. [Hz][c]
Gln2	-91.0	149.6	0.72	0.69	0.70
Ile3	-131.1	138.3	0.87	0.85	0.82
Phe4	-116.0	163.0	0.84	0.77	0.82
Val5	-118.0	140.2	0.76	0.80	0.77
Lys6	-95.2	114.2	0.87	0.73	0.63
Thr7	-99.6	127.5	0.75	0.75	0.67
Leu8	-73.4	170.8	0.43	0.55	0.70
Thr9	-101.4	-6.9	0.24	0.36	0.35
Gly10	77.4	14.9	0.32	0.29	0.33
Lys11	-96.3	16.5	0.43	0.43	0.39
Thr12	-119.9	138.1	0.76	0.81	0.78
Ile13					
Thr14	-101.4	142.0	0.82	0.74	0.72
Leu15	-126.4	139.7	0.79	0.83	0.81
Glu16	-111.8	154.0	0.84	0.77	0.78
Val17	-139.0	121.1	0.87	0.84	0.82
Glu18	-120.0	170.7	0.87	0.78	0.85
Pro19					
Ser20	-79.8	-24.5	0.22	0.23	0.25
Asp21	-71.0	-8.1	0.22	0.26	0.26
Thr22	-83.7	148.4	0.65	0.67	0.68
Ile23	-61.3	160.4	0.43	0.55	0.65
Glu24	-57.6	-37.2	0.03	0.12	0.16
Asn25	-65.5	-40.5	0.11	0.14	0.17
Val26	-58.4	-44.4	0.16	0.11	0.15
Lys27	-60.8	-46.4	0.21	0.11	0.15
Ala28	-66.1	-38.0	0.24	0.15	0.18
Lys29	-64.2	-38.1	0.11	0.14	0.17

Ile30	-70.0	-37.3	0.21	0.16	0.19
Gln31					
Asp32	-53.4	-48.6	0.11	0.09	0.13
Lys33	-93.6	-41.8	0.24	0.25	0.24
Glu34	-123.6	-24.4	0.32	0.40	0.40
Gly35	81.2	-6.3	0.21	0.31	0.29
Ile36	-79.7	5.3	0.38	0.34	0.32
Pro37					
Pro38					
Asp39	-68.2	-32.2	0.10	0.17	0.20
Gln40	-95.8	-15.6	0.38	0.31	0.31
Gln41	-84.8	-10.5	0.27	0.29	0.29
Arg42	-121.2	129.7	0.84	0.81	0.76
Leu43	-103.6	116.0	0.79	0.75	0.66
Ile44	-122.1	130.2	0.92	0.81	0.77
Phe45	-144.3	131.8	0.75	0.87	0.87
Ala46	48.2	129.6	0.65	0.62	0.55
Gly47	61.7	46.0	0.27	0.34	0.37
Lys48	-115.1	21.6	0.54	0.48	0.47
Gln49	-85.8	142.7	0.73	0.69	0.67
Leu50	-79.6	130.3	0.76	0.68	0.62
Glu51	-101.8	138.3	0.84	0.75	0.71
Asp52	-48.2	140.0	0.65	0.58	0.58
Gly53					
Arg54	-85.4	-8.9	0.54	0.30	0.30
Thr55	-104.5	165.5	0.73	0.71	0.78
Leu56	-61.2	164.6	0.27	0.54	0.66
Ser57	-63.9	-36.2	0.10	0.14	0.18
Asp58	-55.6	-29.6	0.05	0.14	0.18
Tyr59	-91.0	-39.3	0.41	0.24	0.24
Asn60	57.9	4.7	0.38	0.24	0.27
Ile61	-88.7	45.4	0.31	0.54	0.44

Gln62	-103.4	116.4	0.71	0.75	0.66
Lys63	-54.8	169.5	0.65	0.50	0.66
Glu64	66.9	143.1	0.76	0.71	0.62
Ser65	-71.1	19.1	0.22	0.38	0.33
Thr66	-119.2	159.5	0.70	0.79	0.82
Leu67					
His68	-105.6	154.6	0.62	0.74	0.76
Leu69	-107.0	135.7	0.85	0.77	0.72
Val70	-108.1	115.8	0.98	0.76	0.68
Leu71	-96.0	139.9	0.60	0.73	0.69
Arg72					
Leu73	-83.7	98.8	0.70	0.69	0.56
Arg74	-97.7	150.4	0.60	0.72	0.72
Gly75	120.4	93.9	0.67	0.64	0.67
Gly76	174.2	125.6	0.75	0.89	1.01

[a] Values of $^{3}J(C_{\alpha},H^{N})$ coupling constants have been determined by taking appropriate ω_3 traces, displacing the two extracted traces with respect to each other and forming the integral of the power difference spectrum as a function of the displacement as described in the text. Coupling constant values are not corrected for $^{13}C_{\alpha}$ spin flips. [b] $^{3}J(C_{\alpha},H^{N})$ coupling constant values predicted by Eq. 4 (2D Fourier series to first order (m = n = 1)) using neighboring ϕ_i and ψ_{i-1} torsion angles of ubiquitin. [c] $^{3}J(C_{\alpha},H^{N})$ coupling constant values predicted by Eq. 3 using neighboring crystallographic ϕ_i and ψ_{i-1} torsion angles of ubiquitin.